ISSN 1070-3284, Russian Journal of Coordination Chemistry, 2020, Vol. 46, No. 8, pp. 545–552. © Pleiades Publishing, Ltd., 2020.
Russian Text © The Author(s), 2020, published in Koordinatsionnaya Khimiya, 2020, Vol. 46, No. 8, pp. 485–492.

The authors congratulate Academician I.L. Eremenko on his 70th jubilee

A Rare Example of Discrete Lanthanide–Lithium Tetrakis-β-Diketonates: Synthesis, Structures, and Luminescence Properties

Yu. S. Kudyakova[a], P. A. Slepukhin[a, b], M. S. Valova[a], Ya. V. Burgart[a, b], V. I. Saloutin[a, b], and D. N. Bazhin[a, b, *]

[a] *Postovsky Institute of Organic Synthesis, Ural Branch, Russian Academy of Sciences, Yekaterinburg, Russia*

[b] *Ural Federal University, Yekaterinburg, Russia*

**e-mail: dnbazhin@gmail.com*

Received December 26, 2019; revised February 13, 2020; accepted February 17, 2020

Abstract—The reactions of functionalized lithium CF_3-β-diketonate (LiL) with europium(III) and terbium(III) chlorides in acetonitrile afford heterobimetallic complexes with the general formula $[LiLnL_4(H_2O)](CH_3CN)$ (Ln = Eu (**IIIa**) and Tb (**IIIb**)). It is found that Ln–Li tetrakis-β-diketonates can also be prepared by the crystallization from acetonitrile of the previously synthesized complexes $[(LnL_3)(LiL)(MeOH)]$ (**I**) and $[(LnL_3)(LiL)(H_2O)]$ (**II**). For the first time, the single crystals of the compounds in a series of Ln–Li tetrakis-β-diketonates are characterized by X-ray diffraction analysis (CIF files CCDC nos. 1973632 (**IIIa**) and 1973633 (**IIIb**)). The photoluminescence properties of the synthesized heterometallic complexes in the solid state are studied.

Keywords: β-diketonates, lanthanides, luminescence, X-ray diffraction analysis

DOI: 10.1134/S1070328420070027

INTRODUCTION

Interest in the complexes based on trivalent lanthanide (Ln) ions is caused by their unique luminescence properties, including the characteristic spectral range, narrow emission bands, and long lifetimes [1–7]. The optimization of the luminescence properties of the Ln(III) complexes requires fine tuning of the molecular structures of the used organic ligands. The intensive use of 1,3-diketones as chelating agents is associated with their efficient binding with metal ions and the possibility to vary the nature of substituents in the dicarbonyl fragment [8–12]. The most promising lanthanide complexes based on 1,3-diketones are tris(diketonates) $Ln(\beta\text{-diketonate})_3(coligand)$ and tetrakis(diketonates) $(cation)Ln(\beta\text{-diketonate})_4$ due to their bright (mechano)luminescence properties [3, 13, 14].

We have previously synthesized the heterobimetallic binuclear complexes $[(LnL_3)(LiL)(MeOH)]$ (**I**) and $[(LnL_3)(LiL)(H_2O)]$ (**II**) (Ln = Eu, Tb, and Dy) based on the earlier prepared lithium CF_3-β-diketonate (LiL) [15]. The structure of the used β-diketonate anion L and its coordination modes are presented in Scheme 1.

The Ln–Li complexes (**I** and **II**) contain four ligand molecules, which, on the one hand, makes them resembling the known lanthanide(III) tetrakis-β-diketonates. On the other hand, the original structure of the complex is formed due to the lanthanide tris-β-diketonate fragment and initial lithium diketonate acting as the coligand. It is important that the additional functional group in the diketonate favors the formation of the heterobimetallic complexes with unique structures [16, 17].

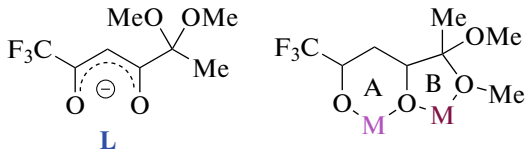

Scheme 1.

An approach to the synthesis of lithium–lanthanide tetrakis-β-diketonates based on the functionalized trifluoromethyl-containing lithium β-diketonate (LiL) is considered and the photoluminescence properties of the new compounds are studied in this work.

EXPERIMENTAL

All procedures related to the synthesis of new complexes were carried out in air using commercial reagents ($EuCl_3 \cdot 6H_2O$ (99.99%), $TbCl_3 \cdot 6H_2O$ (99.99%), and acetonitrile (Alfa Aesar)). Trifluoromethyl-containing lithium β-diketonate LiL was synthesized according to a described procedure [18].

The IR spectra of the compounds were recorded on a Perkin Elmer Spectrum One FT-IR spectrometer in a range of 400–4000 cm^{-1} using a diffuse reflectance accessory for solid substances. Elemental analyses were carried out on a Perkin Elmer PE 2400 Series II automated analyzer.

The photoluminescence properties were studied on a Varian Cary Eclipse fluorescence spectrophotometer. Phosphorescence was measured in the solid phase, and the crystals were deposited on the quartz glass turned by 50° toward the side opposite to the detector window in order to avoid reflections. The mechanoluminescence properties of the synthesized complexes were studied on the same spectrophotometer in the Bio/Chemiluminescence mode grinding the crystals between the quartz glasses.

Synthesis of complexes $[LiLn(L)_4(H_2O)](CH_3CN)$ (Ln = Eu (IIIa) and Tb (IIIb). Salt $LnCl_3 \cdot 6H_2O$ (1 mmol) was added to lithium β-diketonate LiL (4 mmol) in acetonitrile (15 mL). The obtained suspension was heated to boiling and kept until a transparent solution was formed, and then the resulting solution was cooled to room temperature. The slow evaporation of the solvent resulted in the formation of crystals of the complex. The crystals were washed with water and dried in vacuo. The yields of complexes **IIIa** and **IIIb** were 0.90 g (80%) and 0.96 g (85%), respectively.

For $C_{32}H_{42}O_{17}F_{12}LiEu \cdot 0.5\,(CH_3CN)$ (**IIIa**)
(based on 1/2 solvate acetonitrile molecule)

Anal. calcd., %	C, 35.83	H, 3.96	N, 0.63
Found, %	C, 35.47	H, 3.93	N, 0.72

IR (ν, cm^{-1}): 3538, 3489 ν(O–H), 3001, 2948, 2840 ν(C–H), 1654, 1632 ν(C=O), 1613 ν(C=C), 1464, 1436 $\nu_{as}(CH_3)$, 1318–1142 ν(C–F).

For $C_{32}H_{42}O_{17}F_{12}TbLi \cdot (CH_3CN)$ (**IIIb**)

Anal. calcd., %	C, 36.02	H, 4.00	N, 1.24
Found, %	C, 36.11	H, 4.02	N, 1.30

IR (ν, cm^{-1}): 3536, 3494 ν(O–H), 2999, 2949, 2842 ν(C–H), 1652, 1634 ν(C=O), 1614, 1604 ν(C=C), 1468, 1437 $\nu_{as}(CH_3)$, 1316–1140 ν(C–F).

X-ray diffraction analysis (XRD). The crystallographic data for the single crystals of complexes **IIIa** and **IIIb** were obtained on an Xcalibur 3 automated four-circle diffractometer with a CCD detector using a standard procedure (MoK_α radiation, graphite monochromator, ω scan mode with an increment of 1° at $T = 295(2)$ K). An empirical absorption correction was applied. The structure was determined by a direct statistical method and refined by full-matrix least squares for F^2 in the anisotropic approximation for all non-hydrogen atoms. Hydrogen atoms were placed in the geometrically calculated positions and refined in the riding model. All calculations were performed in the Olex program shell [19] using the SHELX program package [20]. The crystallographic data and structure refinement parameters for complexes **IIIa** and **IIIb** are presented in Table 1.

The coordinates of atoms and other parameters for the structures of compounds **IIIa** and **IIIb** were deposited with the Cambridge Crystallographic Data Centre (CIF files CCDC nos. 1973632 and 1973633, respectively; deposit@ccdc.cam.ac.uk or http://www.ccdc.cam.ac.uk/data_request/cif).

RESULTS AND DISCUSSION

The reactions of lithium CF_3-β-diketonate LiL with Eu(III) and Tb(III) chlorides in acetonitrile afford complexes **IIIa** and **IIIb**, respectively, according to reaction (1). Compounds **IIIa** and **IIIb** can also be obtained by the recrystallization from acetonitrile of the corresponding complexes $[(LnL_3)(LiL)(MeOH)]$ (**Ia** and **Ib**) and $[(LnL_3)(LiL)(H_2O)]$ (**IIa** and **IIb**) synthesized earlier [15].

According to the XRD data, binuclear heterometallic complexes **IIIa** and **IIIb** are neutral tetrakis-β-diketonates that crystallize in the centrosymmetric space group $\bar{P}$ of the triclinic system (Fig. 1, Table 1). The Ln(III) atom is octacoordinated due to the oxygen atoms of four diketonate anions. Two ligands are bridging and additionally coordinate the lithium ion via the oxygen atoms μ_2-O(2) and μ_2-O(6) of the 1,3-dicarbonyl fragment. The lithium atom builds up its coordination environment to $[LiO_5]$ due to the O(3) and O(5) oxygen atoms of two methoxy groups and to the O(4) atom of the H_2O molecule. Three ligand molecules of the Ln(III) tetrakis-diketonate fragment exist in the cis position relative to each other.

$$4LiL + LnCl_3 \cdot 6H_2O \xrightarrow{CH_3CN} \underset{\textbf{IIIa, IIIb}}{[LiLnL_4(H_2O)](CH_3CN)} + 3LiCl + 5H_2O \quad (1)$$

Ln = Eu (a), Tb (b)

Table 1. Crystallographic data and structure refinement parameters for compounds **IIIa** and **IIIb**

Parameter	Value	
	IIIa	**IIIb**
FW	1126.61	1133.57
Temperature, K	295(2)	
Crystal system	Triclinic	
Space group	$P\bar{1}$	
a, Å	11.9147(5)	11.8882(2)
b, Å	11.9855(5)	11.9996(5)
c, Å	18.9069(8)	18.8718(7)
α, deg	104.960(4)	105.212(3)
β, deg	96.274(4)	96.109(3)
γ, deg	110.240(4)	110.162(4)
V, Å^3	2387.93(17)	2380.33(17)
Z	2	2
ρ_{calc}, g cm^{-3}	1.567	1.582
μ, mm^{-1}	1.425	1.597
Crystal size, mm	0.46 × 0.39 × 0.27	0.48 × 0.36 × 0.24
θ_{min}–θ_{max}, deg	3.53–31.04	3.54–31.16
F(000)	1132	1136
Ranges of reflection indices	$-14 \le h \le 15$, $-15 \le k \le 16$, $-25 \le l \le 27$	$-11 \le h \le 16$, $-16 \le k \le 17$, $-26 \le l \le 26$
Measured reflections	22441	20712
Independent reflections (R_{int})	12 912 (1132)	13115 (1136)
Number of reflections with $I > 2\sigma(I)$	9051	9544
GOOF	1.055	1.028
R factors for $F^2 > 2\sigma(F^2)$	$R_1 = 0.0604$, $wR_2 = 0.1493$	$R_1 = 0.0595$, $wR_2 = 0.1462$
R factors for all reflections	$R_1 = 0.0905$, $wR_2 = 0.1928$	$R_1 = 0.0853$, $wR_2 = 0.1941$
Residual electron density (max/min), e/Å^3	1.469/–1.984	1.459/–1.925

It can be assumed that the formation of the complex depends on the preferential orientation of four negatively charged β-diketonate anions around the lanthanide(III) ion on going from alcohols (methanol and ethanol) to more polar acetonitrile, whereas complexes **I** and **II** contain the Ln(III) tris-β-diketonate fragment and LiL as the coligand. Thus, the main distinction of complexes **IIIa** and **IIIb** from **IIa** and **IIb** is presented by different organizations of the heterobimetallic framework (Fig. 2).

Note that compounds **IIIa** and **IIIb** are rare examples of lithium–lanthanide tetrakis-β-diketonates, whose structures were determined using the XRD data. The previously synthesized heterobimetallic Ln–Li complexes based on nonfunctionalized β-diketones were assigned to tetrakis-β-diketonates [LiLn(β-diketonate)$_4$] only on the basis of the data of IR spectroscopy and elemental analysis [21, 22].

Unlike other Ln–O distances in complexes **IIIa** and **IIIb**, the bonds with the bridging oxygen atoms Ln–μ_2-O are appreciably longer (Table 2). A systematic decrease in the Ln–O bond lengths is observed on going from europium to terbium caused by the *f*-contraction effect.

According to the data calculated using the SHAPE program [23, 24], the coordination octahedron [LnO$_8$] in complexes **IIIa** and **IIIb** has the geometry of a distorted biaugmented trigonal prism (Table 2), and the [LiO$_5$] pentahedron is a distorted square pyramid.

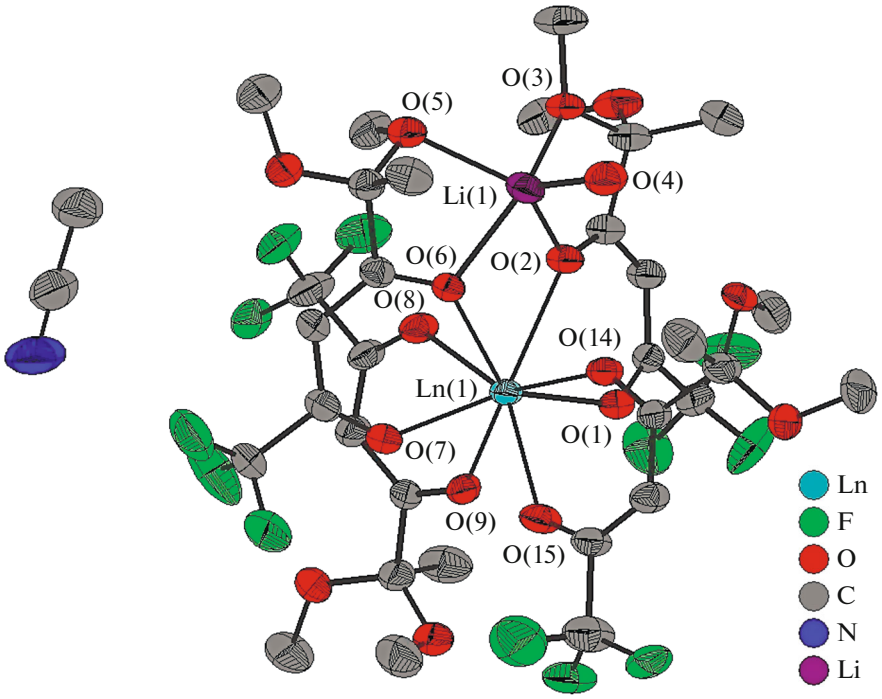

Fig. 1. Molecular structures of complexes **IIIa** (Ln = Eu) and **IIIb** (Ln = Tb) (hydrogen atoms are omitted, thermal ellipsoids of 30% probability).

The mutual intermolecular orientation of the trifluoromethyl groups toward each other (Fig. 3) is a specific feature of the crystal packing of the molecules. The shortest F...F distances are 3.4–3.5 Å. However, the angle between the C–F bonds of the trifluoromethyl groups differs from 90° [25], which does

Table 2. Selected geometric characteristics and phosphorescence lifetimes of the series of the heterometallic binuclear complexes

Complex	Distance, Å				Geometry of $[LnO_8]$**	Phosphorescence lifetime, μs	References
	Ln–O	Ln–μ_2-O	Ln···Ln	Ln···M*			
$[(EuL_3)(LiL)(MeOH)]$ (**Ia**)	2.334–2.533	2.362–2.426	10.527	3.498	TDD-8	732	15
$[(TbL_3)(LiL)(MeOH)]$ (**Ib**)	2.306–2.505	2.350–2.404	10.552	3.471	TDD-8	648	15
$[(EuL_3)(LiL)(H_2O)]$ (**IIa**)	2.346–2.523	2.361–2.412	9.613	3.508	TDD-8	642	15
$[(TbL_3)(LiL)(H_2O)]$ (**IIb**)	2.320–2.503	2.330–2.389	9.923	3.494	TDD-8	520	15
$[LiEuL_4(H_2O)](CH_3CN)$ (**IIIa**)	2.352–2.389	2.420–2.461	9.560	3.568	BTRP-8	576	
$[LiTbL_4(H_2O)](CH_3CN)$ (**IIIb**)	2.344–2.368	2.398–2.448	9.545	3.535	BTRP-8	480	
$Na[TbL_4](MeOH)(H_2O)$ (**IV**)	2.323–2.400	2.375–2.384	11.658	3.784	TDD-8	640	16
$K[TbL_4](H_2O)$ (**V**)	2.331–2.401	2.377-2.393	10.455	4.047	TDD-8	292	16
$Cs[TbL_4]$ (**VI**)	2.308–2.363	2.410–2.421	10.995	4.456, 4.505	SAPR-8	48	16

* M is alkali metal (Li, Na, K, and Cs).
** According to the data calculated using the SHAPE program (TDD-8 is trigonal dodecahedron, BTRP-8 is biaugmented trigonal prism, and SAPR-8 is square antiprism).

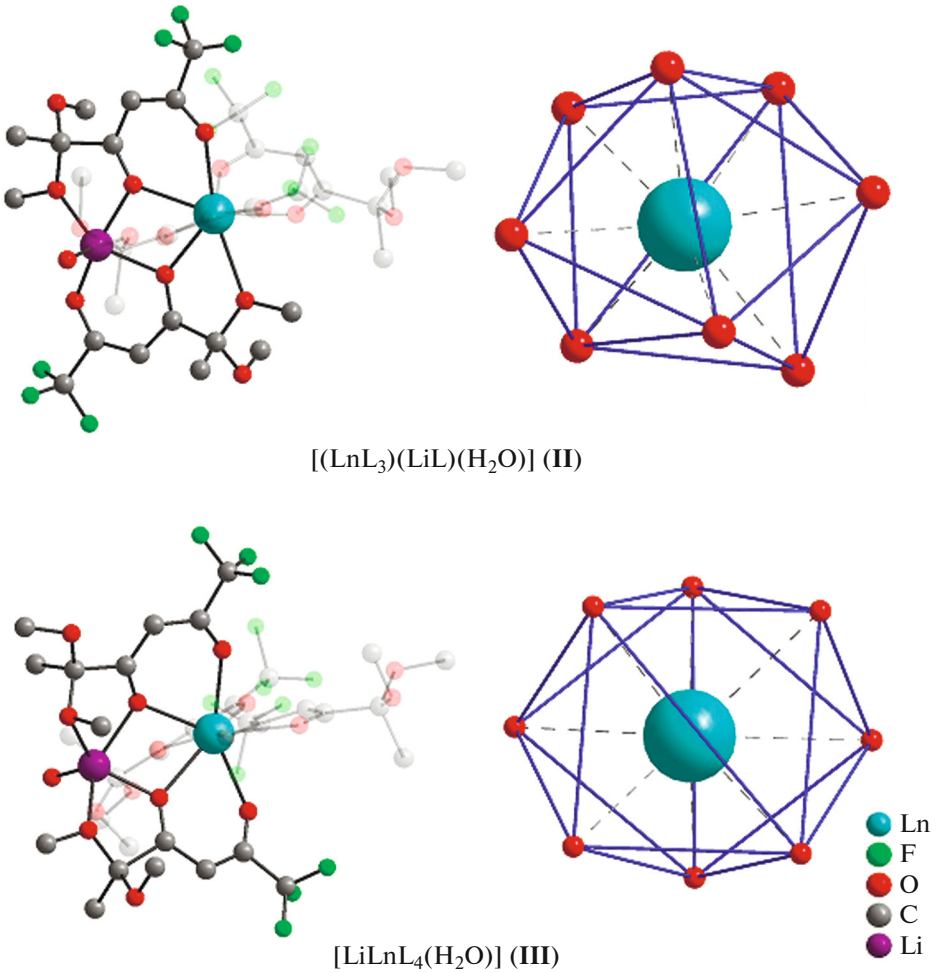

Fig. 2. Differences in the organization of the heterobimetallic framework and geometry of the coordination polyhedra LnO_8 in tris(β-diketonates) $[(LnL_3)(LiL)(H_2O)]$ **II** [15] and tetrakis(β-diketonates) $[LiLnL_4(H_2O)]$ **III**.

not allow one to consider these bonds as the true halogen–halogen interaction. The Ln–Ln distances between the adjacent molecules are close to those found for complexes **IIa** and **IIb** (Table 2). In complexes **IIIa** and **IIIb**, the water molecule coordinated to the lithium ion forms hydrogen bonds of two types: the intramolecular hydrogen bond with the O(16) oxygen atom of the methoxy group and the intermolecular hydrogen bond with the solvate acetonitrile molecule (Fig. 3, Table 3).

The photoluminescence properties of compounds **IIIa** and **IIIb** were studied in the solid state. The absorption spectra of complexes **IIIa** and **IIIb** exhibit absorption maxima at wavelengths of 338 and 343 nm, respectively (Fig. 4). Using these wavelengths, we recorded the photoluminescence spectra of com-

Table 3. Geometric parameters of hydrogen bonds in complexes **IIIa** and **IIIb**

Complex	D–H···A	Distance, Å			∠DHA, deg	Symmetry
		D···H	H···A	D···A		
IIIa	O(4)–H(4*A*)···N(1)	0.862	2.054	2.889	163.01	$x-1, y, z$
	O(4)–H(4B)···O(16)	0.860	2.258	2.964	139.28	
IIIb	O(4)–H(4*A*)···N(1)	0.858	2.061	2.902	166.65	$x-1, y, z$
	O(4)–H(4*B*)···O(16)	0.858	2.139	2.967	161.97	

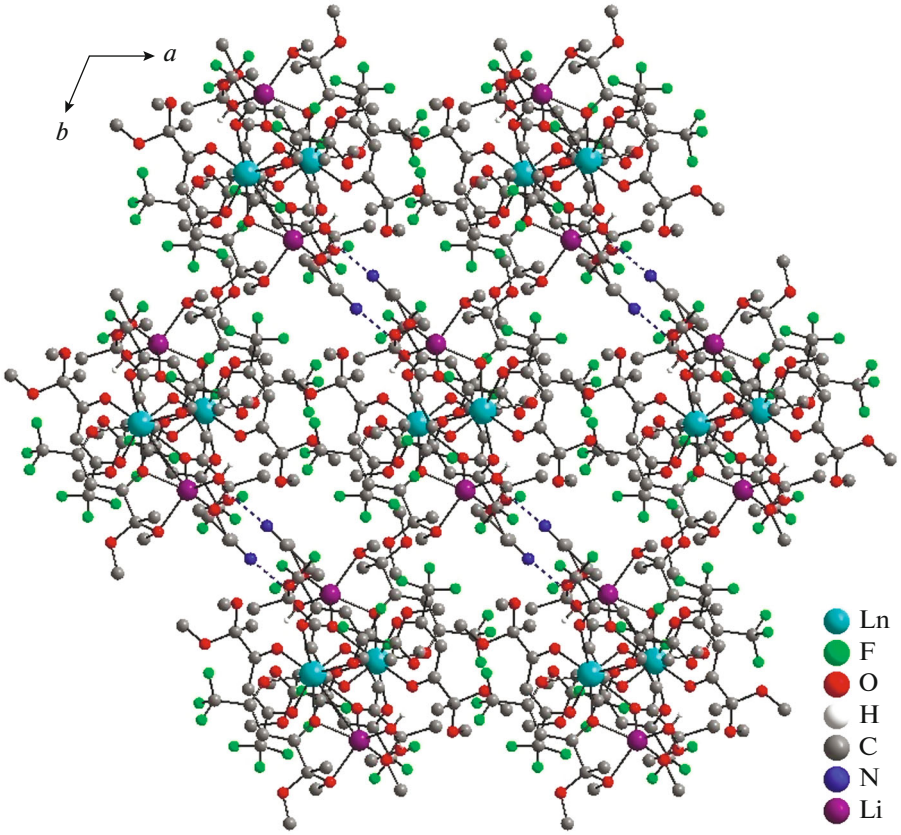

Fig. 3. Molecular packing of complexes **IIIa** and **IIIb** along the *c* axis. Hydrogen atoms (except for the H(4*A*) and H(4*B*) atoms of the water molecule) are omitted. Intermolecular hydrogen bonds are shown by dash.

pounds **IIIa** and **IIIb** containing the metal-centered emission bands characteristic of europium(III) and terbium(III) ions and induced by the *f*–*f* transitions (Table 4). A series of heterobimetallic Ln–M complexes (M = Li, Na, K, and Cs) **I**–**VI** synthesized from functionalized CF_3-β-diketonate L [15, 16] is presented in Table 2. The variation of the alkali metal ion and crystallization conditions leads to a change in the symmetry of the coordination polyhedron around the Ln(III) ion and the nature of the ligand field, which, in turn, affects the photoluminescence spectra of the complexes [26]. As compared to compounds **Ia**, **Ib**, **IIa**, **IIb**, and **IV**, the phosphorescence lifetimes of complexes **IIIa** and **IIIb** decrease: on the one hand, it is likely the result of a change in the geometry of the $[TbO_8]$ polyhedron from the trigonal dodecahedron to the biaugmented trigonal prism (Table 2). On the other hand, the transition from polymeric potassium and cesium terbium(III) tetrakis(diketonates) **V** and **VI** to complexes **I**, **III**, and **IV** leads to a longer afteremission, which is caused by a decrease in the nonradiative transitions propability in the case of discrete structures. Therefore, the photoluminescence properties of Ln–M diketonates depend on a set of factors: the coordination environment around the lanthanide ion, alkali metal nature, and intermolecular organization of the heterometallic complexes.

We have previously established a relationship between the crystal packing of complexes **Ia**, **Ib**, **IIa**, and **IIb** and the mechanoluminescence properties of the diketonates [15, 16]. Similarly to the $[(LnL_3)(LiL)(H_2O)]$ complexes (**IIa** and **IIb**), the intermolecular hydrogen interactions is a reason for the absence of luminescence upon the mechanical destruction of the crystals of complexes **IIIa** and **IIIb** (Table 3). This observation confirms the determining effect of the intermolecular organization of the complexes in the crystalline state on their mechanoluminescence properties [27]. The presence of the interlayer space, so-called cleavage planes, enables the displacement/decomposition of the crystal structure along these planes under the mechanical action thereby inducing luminescence similar to the luminescence spectrum of the substance [28, 29]. In the synthesized complexes **I**–**III**, the Ln–Ln distance (shorter than 10 Å) is an indicator of a denser crystal packing in which intermolecular hydrogen interactions occur due to the close distance between the layers.

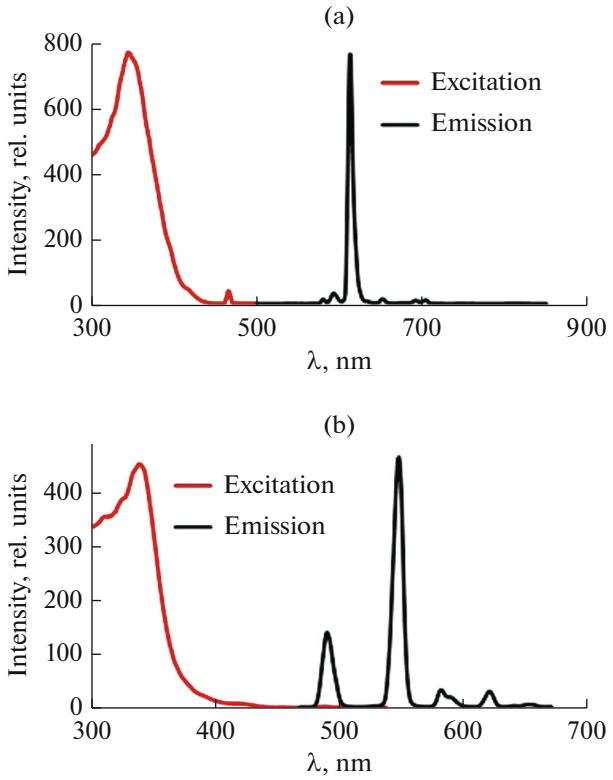

Fig. 4. Photoluminescence spectra of solid complexes (a) **IIIa** (λ_{exc} = 338 nm) and (b) **IIIb** (λ_{exc} = 343 nm) at room temperature.

It is shown in this work that the reactions of functionalized lithium CF_3-β-diketonate with trivalent europium and terbium salts in acetonitrile afford lithium–lanthanide tetrakis(β-diketonates). The XRD data indicate that the presence of the acetal group in the ligand structure determines the coordination of the lithium ion to the ligand and the formation of the discrete structure of the complex. The dependences of the photoluminescence properties of the coordination environment of lanthanide, alkali metal nature, and specific features of the crystal packing were revealed in the series of heterometallic (Ln–M)-β-diketonates (M is alkali metal).

ACKNOWLEDGMENTS

The XRD and physicochemical studies were carried out using the equipment of the Center for Collective Use "Spectroscopy and Analysis of Organic Compounds" on the basis of the Postovsky Institute of Organic Synthesis (Ural Branch, Russian Academy of Sciences).

FUNDING

This work was supported by the Russian Foundation for Basic Research (project no. 18-33-20124), Council for Grants of President of the Russian Federation (grant no. MK-1453.2019.3), and basic themes of the Russian Academy of Sciences (state registration nos. AAAA-A19-119011790132-7 and AAAA-A19-119012490006-1).

CONFLICT OF INTEREST

The authors declare that they have no conflicts of interest.

Table 4. Photoluminescence data for complexes **IIIa** and **IIIb**

Ln(III)	Electronic transitions	Wavelength, nm	Emission band intensity, %
Eu	$^5D_0 \rightarrow {}^7F_6$	580	1.3
	$^5D_0 \rightarrow {}^7F_5$	592	4.6
	$^5D_0 \rightarrow {}^7F_4$	613	91.6
	$^5D_0 \rightarrow {}^7F_3$	652	2.0
	$^5D_0 \rightarrow {}^7F_1$	750	0.5
Tb	$^5D_0 \rightarrow {}^7F_6$	490	18.1
	$^5D_0 \rightarrow {}^7F_5$	546	66.4
	$^5D_0 \rightarrow {}^7F_4$	582	6.1
	$^5D_0 \rightarrow {}^7F_3$	621	4.0
	$^5D_0 \rightarrow {}^7F_2$	650	0.8

REFERENCES

1. Kovacs, D. and Borbas, K.E., *Coord. Chem. Rev.*, 2018, vol. 364, p. 1.
2. Xu, H., Sun, Q., An, Z., et al., *Coord. Chem. Rev.*, 2015, vols. 293–294, p. 228.
3. Bünzli, J.-C.G., *Coord. Chem. Rev.*, 2015, vols. 293–294, p. 19.
4. Bünzli, J.-C.G., *J. Lumin.*, 2016, vol. 170, p. 866.
5. Balashova, T.V., Rumyantsev, R.V., Fukin, G.K., et al., *Russ. J. Coord. Chem.*, 2017, vol. 43, p. 852. https://doi.org/10.1134/S1070328417120016
6. Yuan, C.M., Hu, X., Li, Y., et al., *Russ. J. Coord. Chem.*, 2019, vol. 45, p. 824. https://doi.org/10.1134/S1070328419110113
7. Kharcheva, A.V., Borisova, N.E., Ivanov, A.V., et al., *Russ. J. Inorg. Chem.*, 2018, vol. 63, p. 219. https://doi.org/10.1134/S0036023618020092
8. Brock, A.J., Clegg, J.K., Li, F., and Lindoy, L.F., *Coord. Chem. Rev.*, 2018, vol. 375, p. 106.
9. Mishra, S. and Daniele, S., *Chem. Rev.*, 2015, vol. 115, p. 8379.
10. Vigato, P.A., Peruzzo, V., and Tamburini, S., *Coord. Chem. Rev.*, 2009, vol. 253, p. 1099.
11. Condorelli, G.G., Malandrino, G., and Fragala, I.L., *Coord. Chem. Rev.*, 2007, vol. 251, p. 1931.
12. Kudyakova, Y.S., Bazhin, D.N., Burgart, Y.V., and Saloutin, V.I., *Mendeleev Commun.*, 2016, vol. 26, p. 54.
13. Eliseeva, S.V. and Bünzli, J.-C.G., *Chem. Soc. Rev.*, 2010, vol. 39, p. 189.
14. Binnemans, K., *Chem. Rev.*, 2009, vol. 109, p. 4283.
15. Bazhin, D.N., Kudyakova, Y.S., Bogomyakov, A.S., et al., *Inorg. Chem. Front*, 2019, vol. 6, p. 40.
16. Kudyakova, Yu.S., Slepukhin, P.A., Valova, M.S., et al., *Eur. J. Inorg. Chem.*, 2020, no. 6, p. 523.
17. Krisyuk, V.V., Urkasymkyzy, S., Rybalova, T.V., et al., *J. Coord. Chem.*, 2018, vol. 71, p. 2194.
18. Bazhin, D.N., Chizhov, D.L., Röschenthaler, G.-V., et al., *Tetrahedron Lett.*, 2014, vol. 55, p. 5714.
19. Dolomanov, O.V., Bourhis, L.J., Gildea, R.J., et al., *J. Appl. Crystallogr.*, 2009, vol. 42, p. 339.
20. Sheldrick, G.M., *Acta Crystallogr., Sect. A: Found. Crystallogr.*, 2008, vol. 64, p. 112.
21. Priya, J., Gondia, N.K., Kunti, A.K., and Sharma, S.K., *ECS J. Solid State Sci. Tech.*, 2016, vol. 5, p. R166.
22. Teixeira, K.C., Moreira, G.F., Quirino, W.G., et al., *J. Therm. Anal. Calorim.*, 2011, vol. 106, p. 587.
23. Casanova, D., Llunell, M., Alemany, P., and Alvarez, S., *Chem.-Eur. J.*, 2005, vol. 11, p. 1479.
24. Llunell, M., Casanova, D., Cirera, J., et al., *SHAPE. Version 2.1*, Barcelona: Electronic Structure Group Univ. de Barcelona, 2013.
25. Reichenbächer, K., Süss, H.I., and Huliger, J., *Chem. Soc. Rev.*, 2005, vol. 34, p. 22.
26. Binnemans, K., *Handbook on the Physics and Chemistry of Rare Earths*, Elsevier, 2005, vol. 35, p. 107.
27. Bünzli, J.-C.G. and Wong, K.-L., *J. Rare Earths*, 2018, vol. 36, p. 1.
28. Bukvetskii, B.V., Mirochnik, A.G., and Zhikhareva, P.A., *Luminescence*, 2017, vol. 27, p. 773.
29. Bukvetskii, B.V., Shishov, A.S., and Mirochnik, A.G., *Luminescence*, 2016, vol. 31, p. 1329.

Translated by E. Yablonskaya